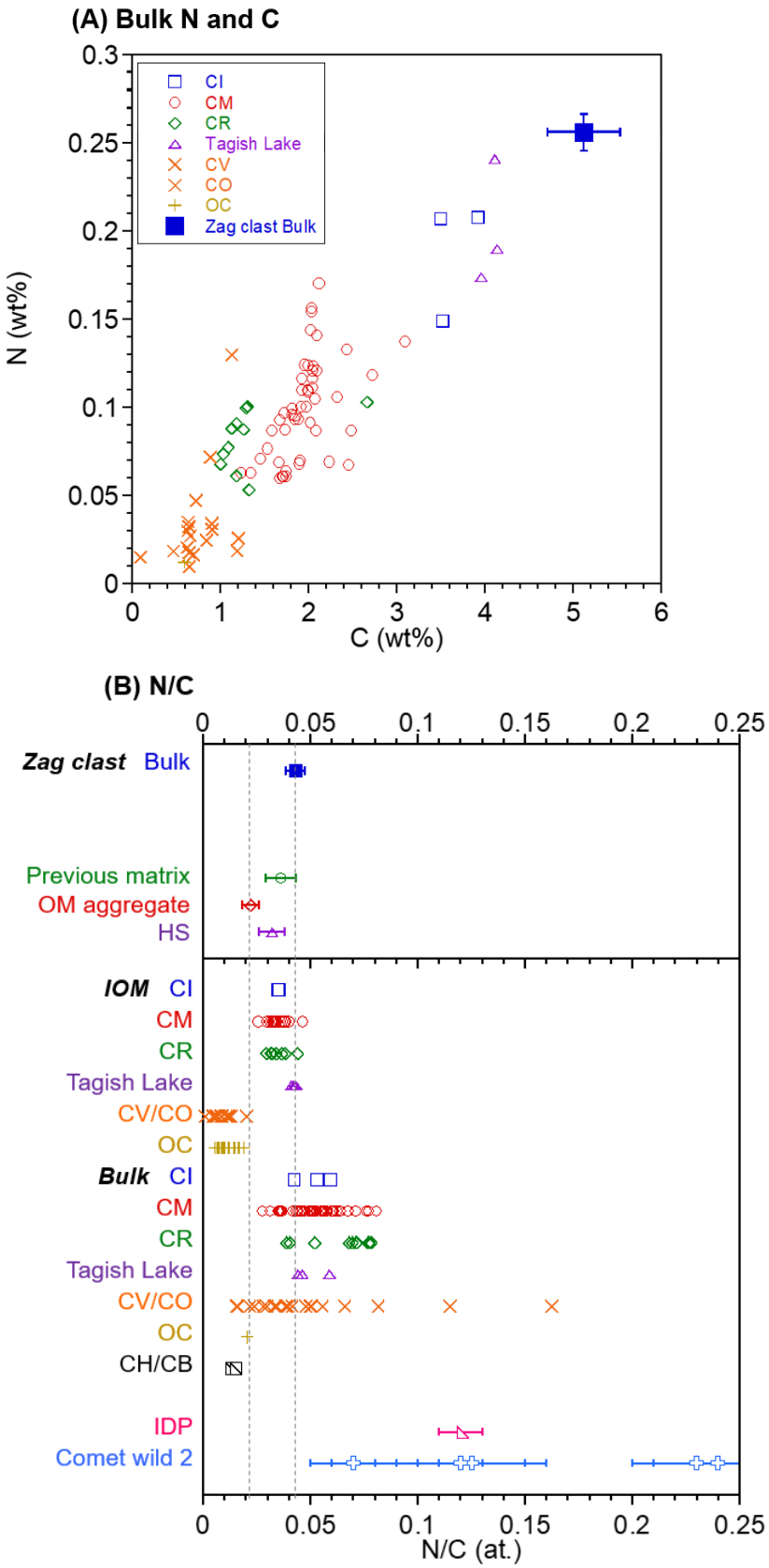

Fig. 1. (A) The bulk C and N abundances (wt.%) of the Zag clast, and various carbonaceous chondrites. (B) The N/C ratios of the Zag clast, various chondrites (bulk and IOM), an IDP, and Comet Wild 2. Chondrite, IDP, and cometary particle data from: Grady and Pillinger (1990); Alexander et al. (2007); Cody et al. (2008); Ivanova et al. (2008); Alexander et al. (2010); De Gregorio et al. (2010); Herd et al. (2011); Alexander et al. (2012); Alexander et al. (2018).

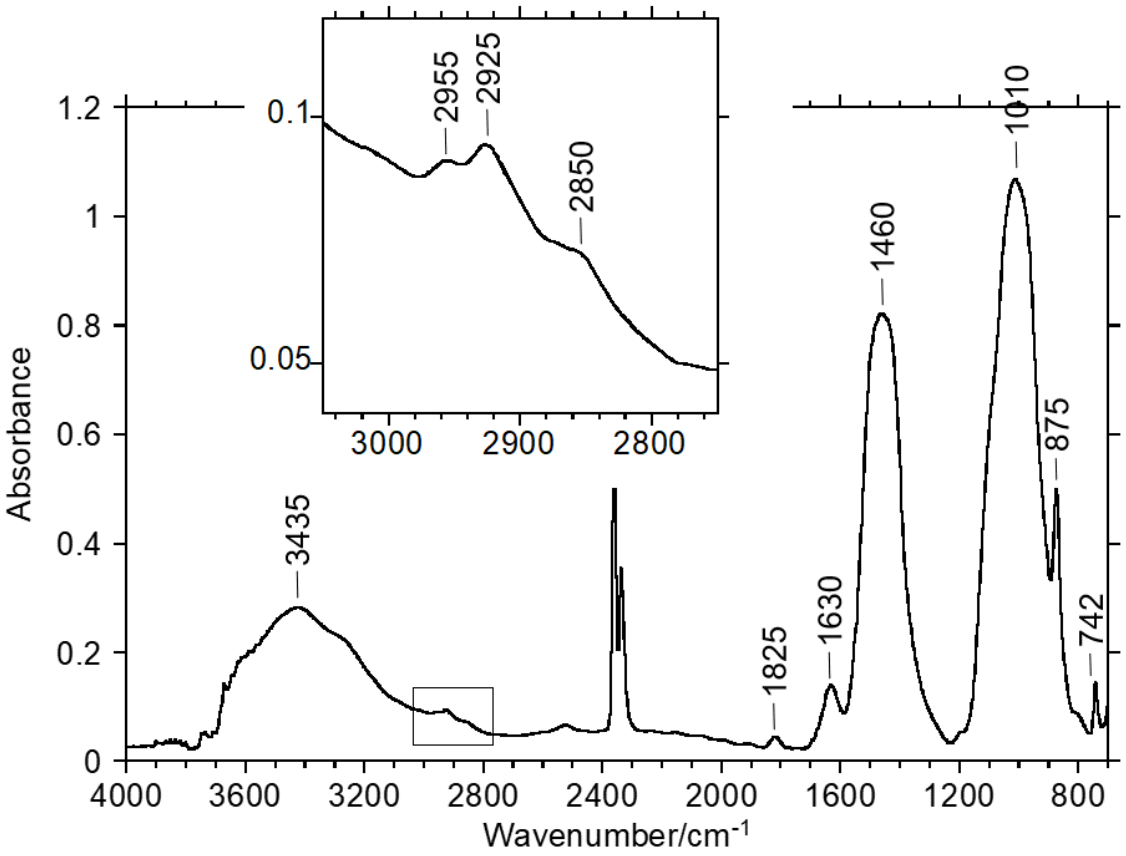

Fig. 2. Infrared absorption spectrum of the clast from the Zag meteorite.

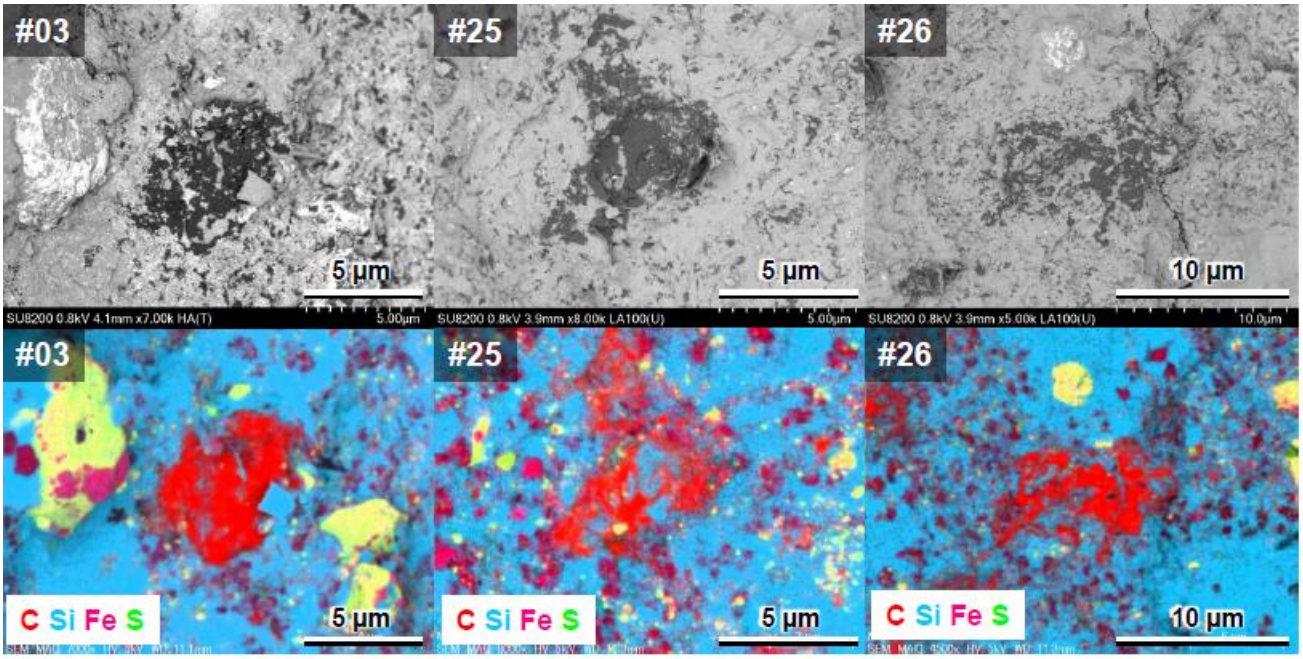

Fig. 3. (Upper) Backscattered electron (BSE) images of the carbon-rich areas in the Zag clast. (Lower) Elemental composition maps by energy-dispersive X-ray spectroscopy (EDS) of the carbon-rich areas in the Zag clast.

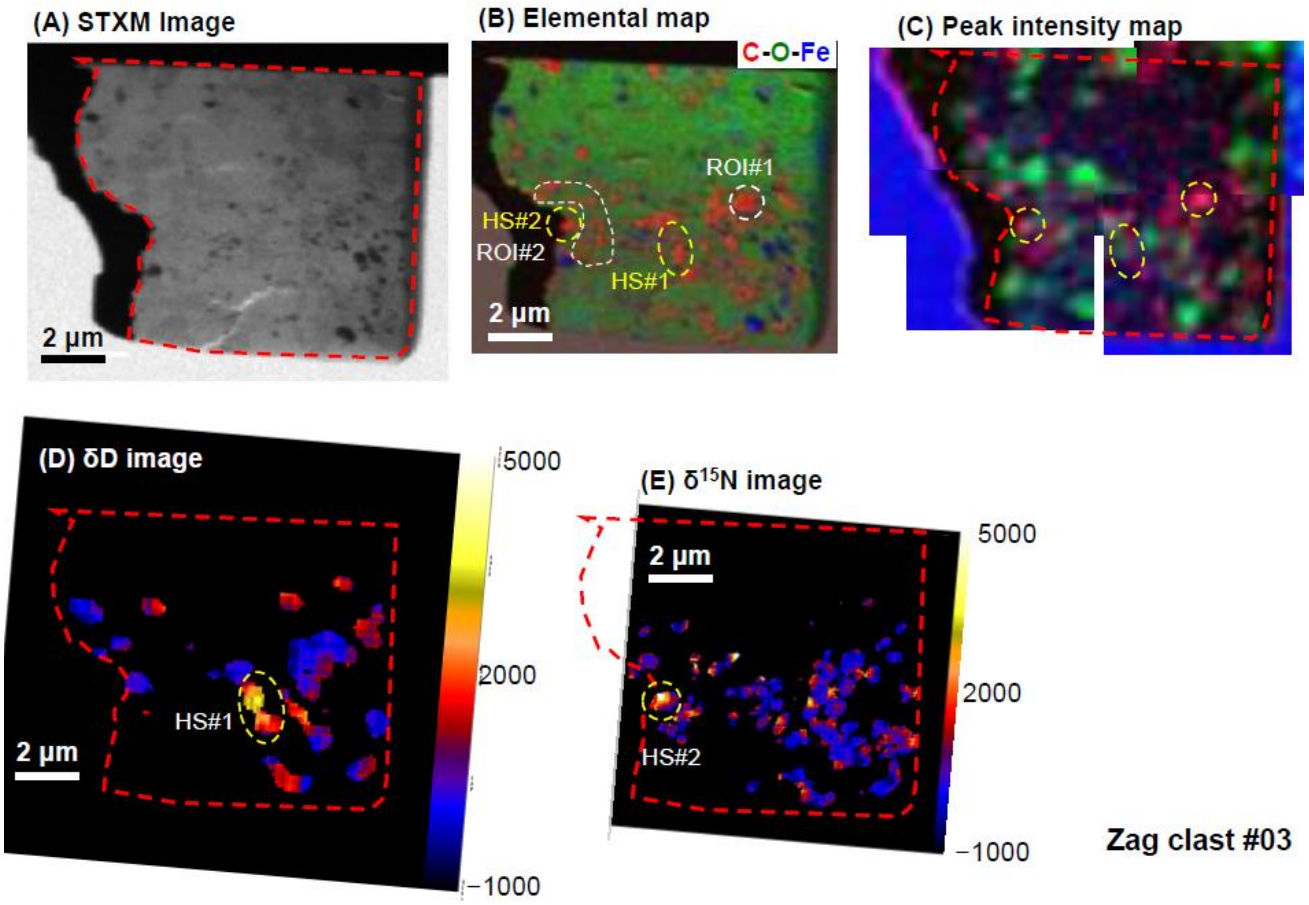

Fig. 4. The FIB section from the C-rich area #03 in the Zag clast. (A) A STXM image at 395 eV (darker area corresponds to lower transmission), (B) C-O-Fe elemental map, (C) Peak intensity map, aromatic C in red, carbonates in green, and blue corresponds to background, (D) δD image, and (E) $\delta^{15}N$ image. Yellow circles indicate δD and $\delta^{15}N$ hot spots.

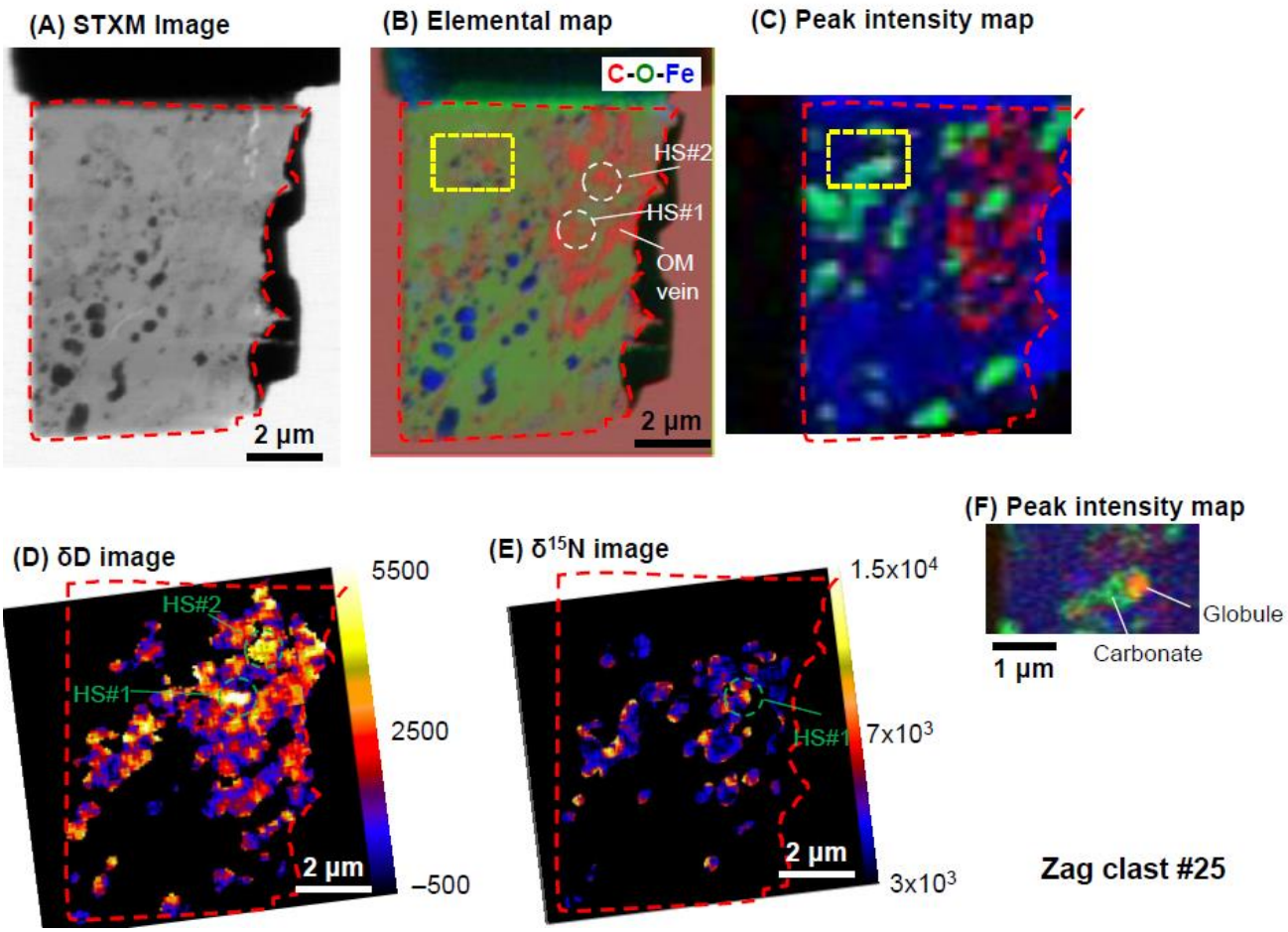

Fig. 5. The FIB section from the C-rich area #25 in the Zag clast. (A) A STXM image at 395 eV (darker area corresponds to lower transmission), (B) C-O-Fe elemental map, (C) Peak intensity map, aromatic C in red, carbonates in green, and blue corresponds to background, (D) δD image, and (E) $\delta^{15}N$ image. A yellow rectangle contained an organic nanoglobules. An enlarged peak intensity map of the yellow rectangle area is shown in (E).

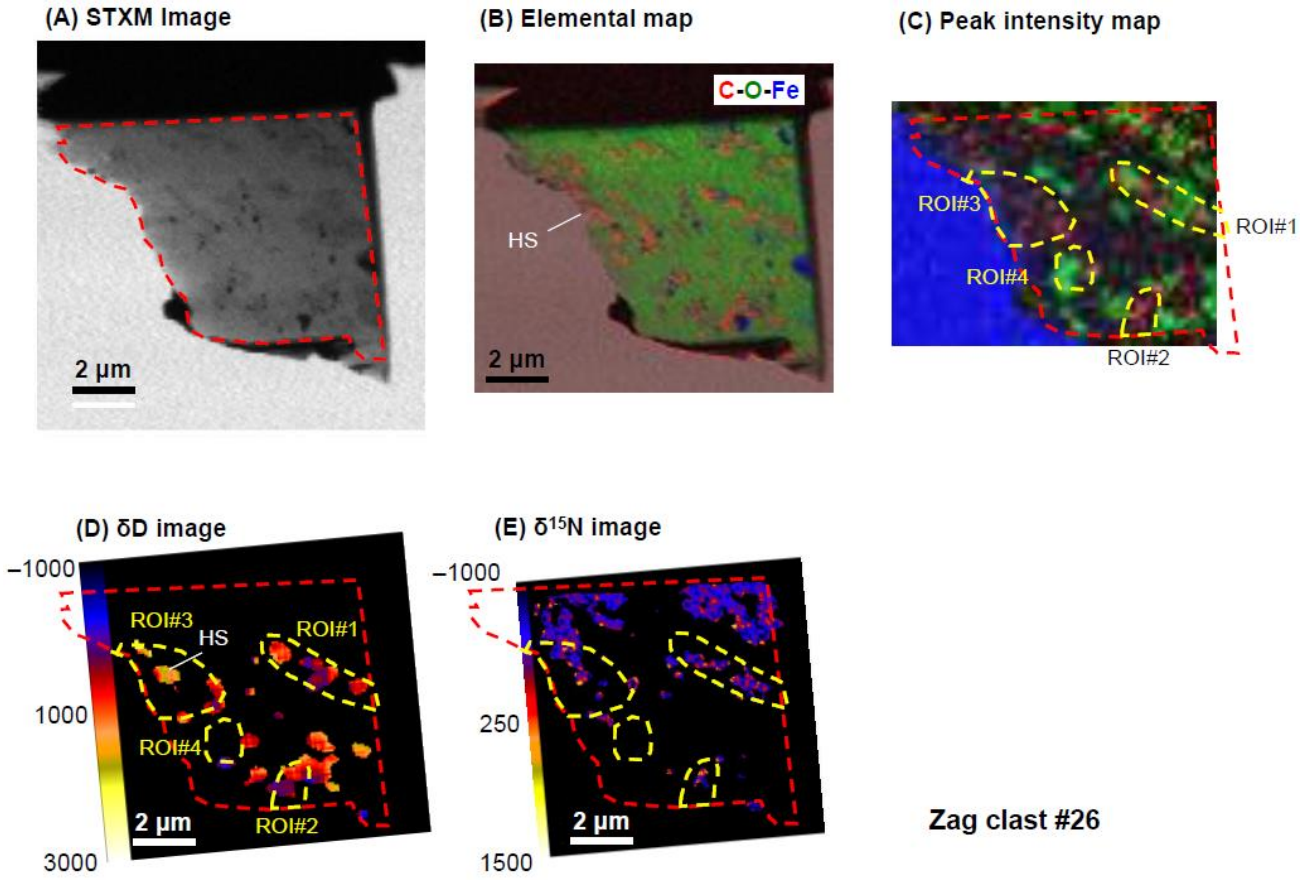

Fig. 6. The FIB section from the C-rich area #26 in the Zag clast. (A) A STXM image at 395 eV (darker area corresponds to lower transmission), (B) C-O-Fe elemental map, (C) Peak intensity map, aromatic C in red, carbonates in green, and blue corresponds to background, (D) δD image, and (E) $\delta^{15}N$ image.

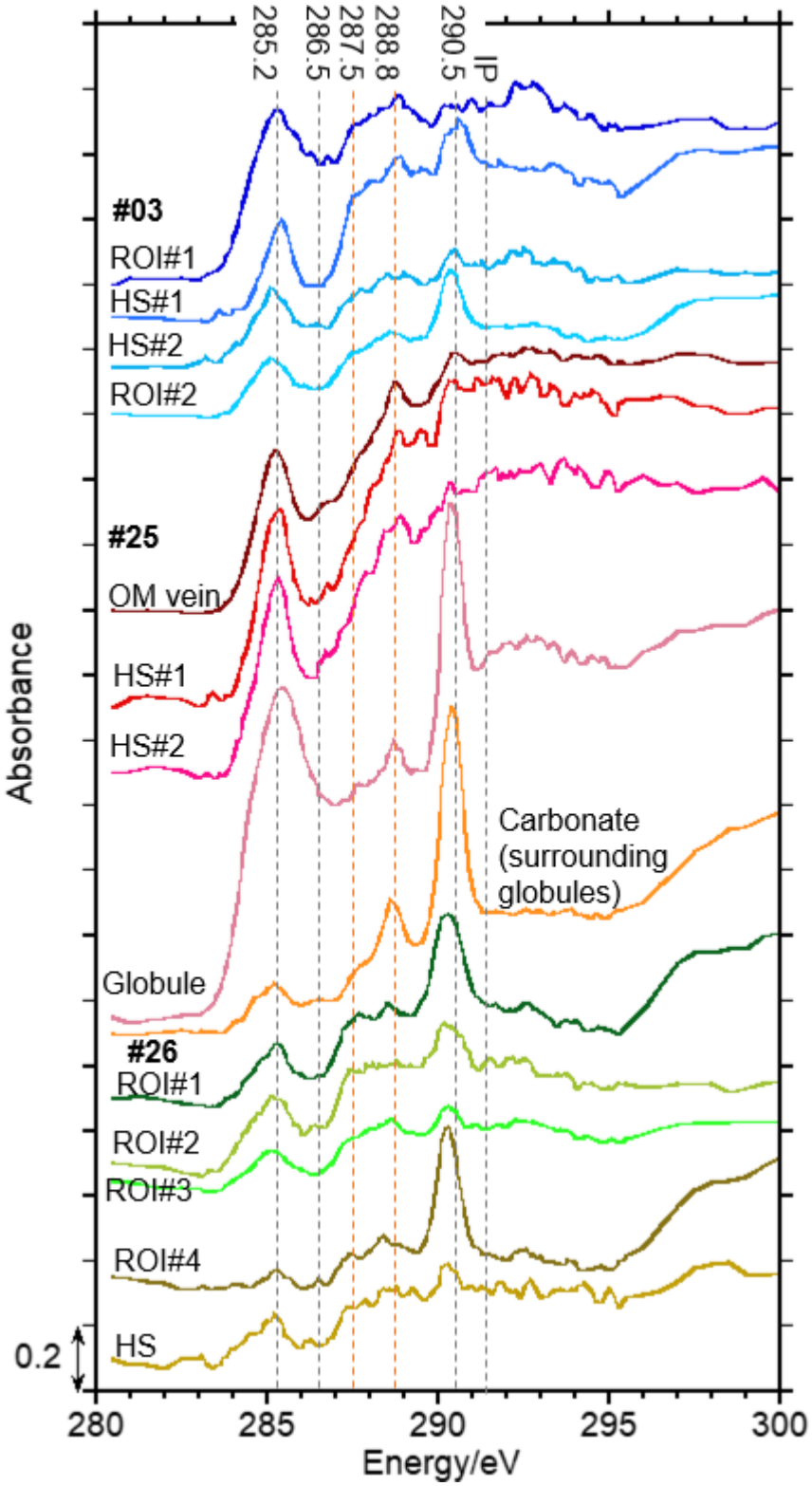

Fig. 7. The C-XANES spectra of the Zag clast FIB sections #03, #25 and #26. The spectra were obtained from regions shown in Figs. 4-6.

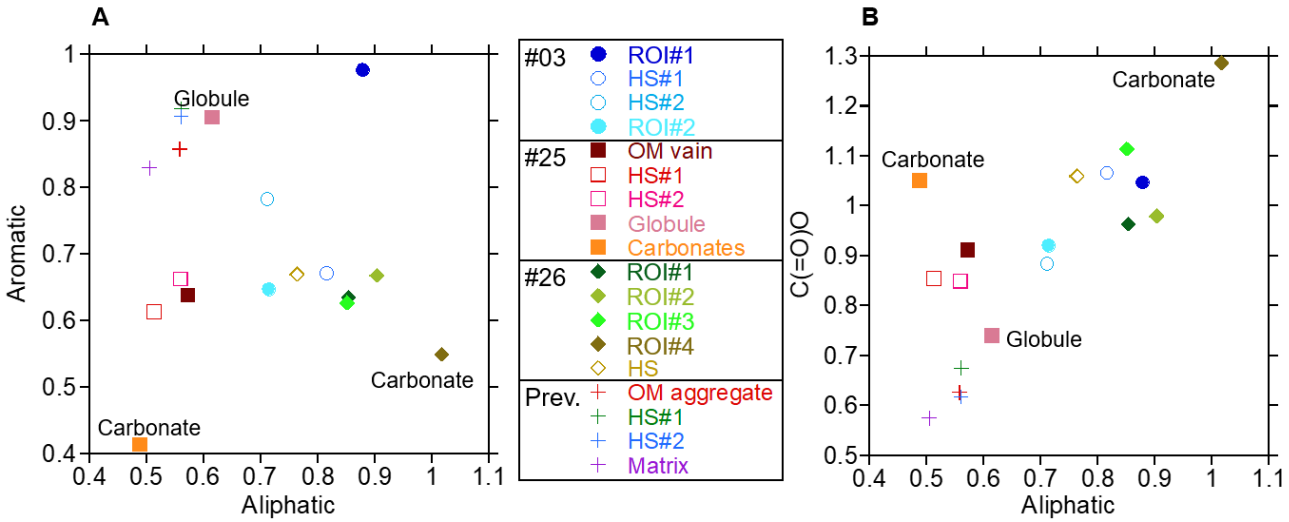

Fig. 8. The C-XANES peak intensities normalized by the intensities at 291.5 eV. (A) Aliphatic vs. aromatic, (B) aliphatic vs. C(=O)O.

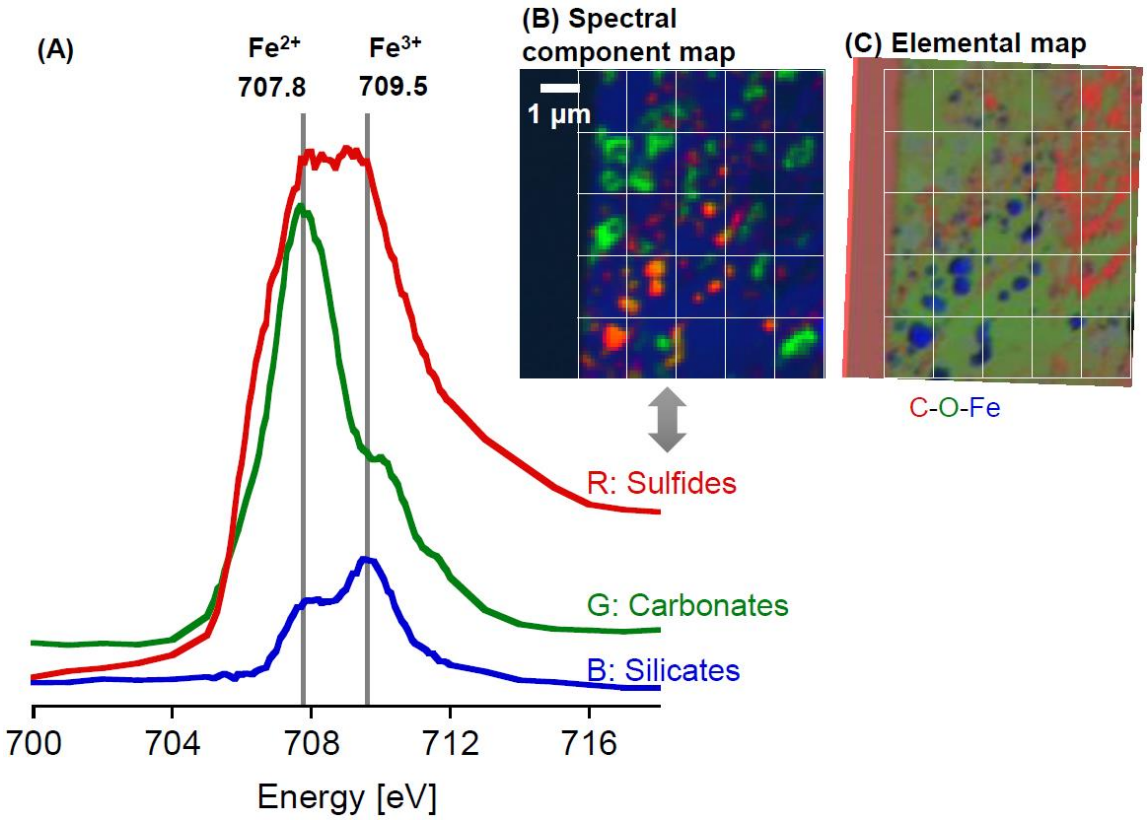

Fig. 9. (A) The Fe-XANES spectra of the Zag clast FIB section #25. (B) The spectral component map generated from the spectra shown in (A). Red region corresponds to Fe-rich nodules, green region corresponds to carbonates, and blue region corresponds to the matrix. (C) The C-O-Fe elemental map (same as Fig. 4B) was shown next to the composition map for comparison.

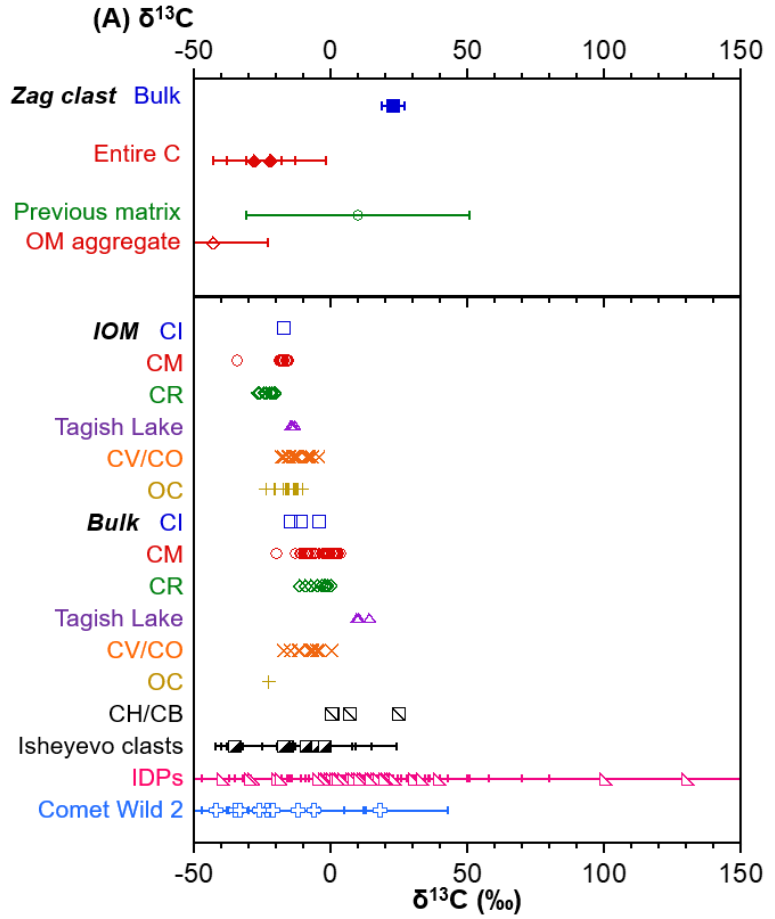
(A) δ13C
-50
0
50
100
150
Zag clast Bulk
Entire C
Previous matrix
OM aggregate
IOM CI
CM
CR
Tagish Lake
CV/CO
OC
Bulk CI
CM
CR
Tagish Lake
CV/CO
OC
CH/CB
Isheyevo clasts
IDPs
Comet Wild 2
δ13C (‰)

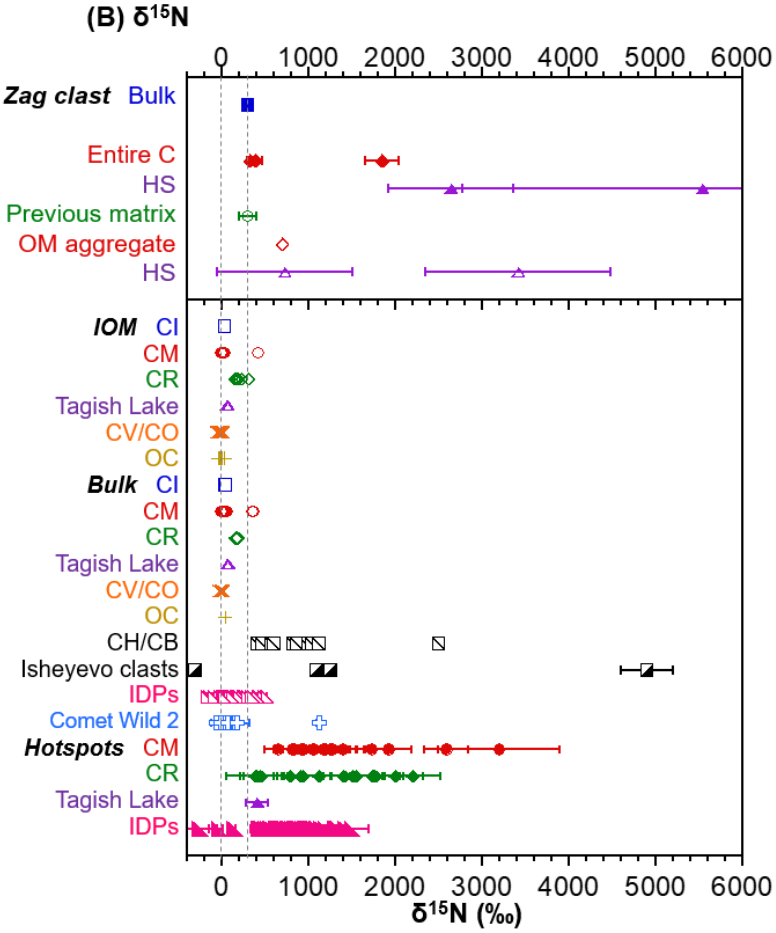
(B) δ15N
0
1000
2000
3000
4000
5000
6000
Zag clast Bulk
Entire C
HS
Previous matrix
OM aggregate
HS
IOM CI
CM
CR
Tagish Lake
CV/CO
OC
Bulk CI
CM
CR
Tagish Lake
CV/CO
OC
CH/CB
Isheyevo clasts
IDPs
Comet Wild 2
Hotspots CM
CR
Tagish Lake
IDPs
δ15N (‰)

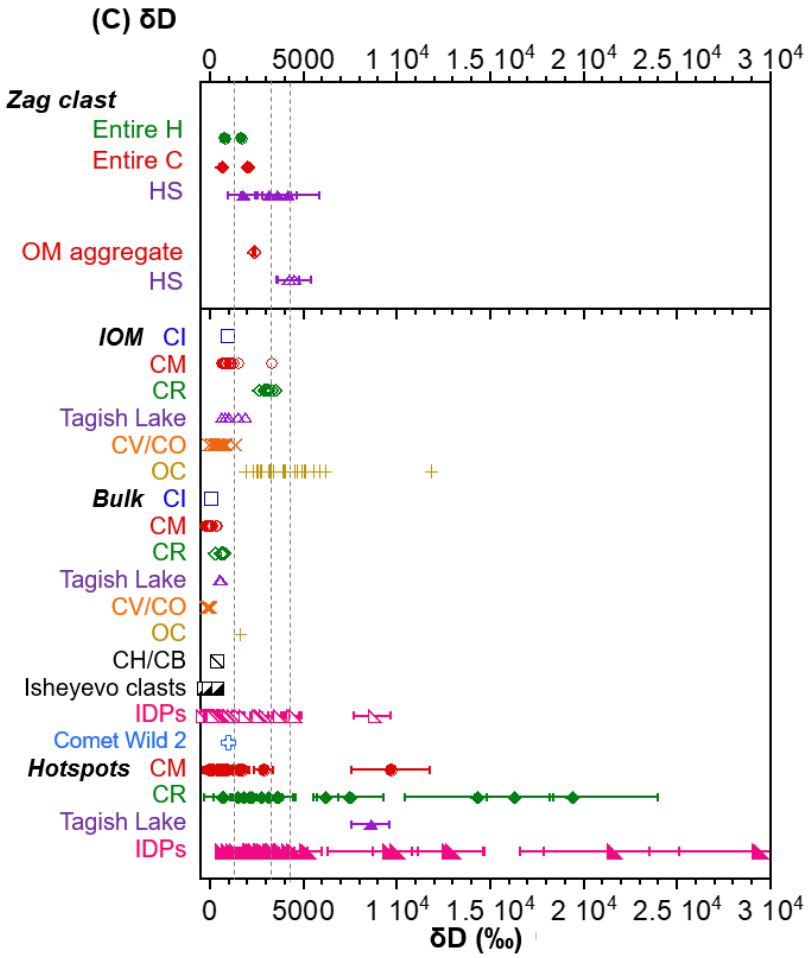

Fig. 10. The isotopic compositions of the Zag clast comparing to various chondrites, IDPs and cometary particles. (A) The C isotopic compositions, (B) the N isotopic compositions, and (C) the H isotopic composition. Data: IOM, Alexander et al. (2007); Alexander et al. (2010); Tagish Lake IOM, Herd et al. (2011), Bulk chondrites, Alexander et al. (2012); Alexander et al. (2018); CH/CB, Prombo and Clayton (1985); Franchi et al. (1986); Grady and Pillinger (1990, 1993); Sugiura and Zashu (2001); Ivanova et al. (2008); Briani et al. (2009); Bonal et al. (2010); IDPs, Floss et al. (2006, 2011); Busemann et al. (2009); Davidson et al. (2012); Hotspots, Busemann et al. (2006); Hashiguchi et al. (2015); Comet 81P/Wild 2, De Gregorio et al. (2010); De Gregorio et al. (2011); Matrajt et al. (2013).